

Some Calculations on Coupling Between Satellite Communications and Terrestrial Radio-Relay Systems Due to Scattering by Rain

By L. T. GUSLER and D. C. HOGG

(Manuscript received March 9, 1970)

Interference coupling due to rain is an important factor in coordinating the shared use of frequencies between satellite-communications and terrestrial microwave radio-relay systems. Calculations of the coupling between a satellite ground station and a radio-relay station due to scattering by rain are given for the frequencies 4, 6, 11, 18.5 and 30 GHz. Several models of the rain environment are considered, one in which the rain falls uniformly over the path, and others involving localized showers in the earth-station beam. The beam of the earth-station antenna is taken to be elevated 30° above the local horizon. Interstation distances from 5 km to 200 km and rain rates up to 400 mm/hr are considered. The analysis includes the near field of the earth-station antenna and shows that attenuation by the rain on the path plays an important role at the higher frequencies. The greatest coupling occurs when the beam of the earth-station antenna is pointed opposite to the azimuth of the relay station. In that case, when the radio-relay antenna response in the direction of the earth station is isotropic, the maximum couplings are -132 dB and -164 dB at 4 GHz with separations of 5 km and 200 km respectively, for a rain rate of 400 mm/hr.

I. INTRODUCTION

Sharing of microwave bands by terrestrial and satellite-communication systems has stimulated investigation of the factors which lead to mutual interference. Of course, antenna characteristics are of prime importance; very low immediate and far side lobes in the antenna

radiation patterns are mandatory in reducing coupling between stations of the two systems. However, even with ideal antennas, there are certain propagation mechanisms that can introduce coupling, one being scatter by precipitation, in particular, rain.

Much knowledge of scattering by rain has been gained through studies with weather radar.¹ Relationships between the backscattering coefficient, the size of the raindrops, the rain rate, and the radio wavelength have been established. These commonly accepted relationships are used in our calculation. Attenuation by the rain is also germane to the calculation, especially at frequencies exceeding 10 GHz, because power from one station that is scattered by a particular volume of rain may well pass through additional precipitation before reaching the other station. The attenuation constants used here are based on measurements with terrestrial systems;² for high rain rates they agree with calculations using the Mie theory with a Laws-Parsons drop-size distribution.

In these calculations, the satellite-communications antenna is assumed to be large in terms of wavelengths and to have a well-tapered quasi-gaussian illumination. As mentioned above, the latter is necessary in practice to produce low immediate and far side-lobe levels. However, this assumption is also advantageous because when the antenna illumination taper is taken to be gaussian, the radiation pattern is readily described analytically at any cross section along the beam from the aperture to infinity.^{3,4} This is an important factor because the "near-field zone" of a large space communication antenna may extend for miles; the coupling due to scattering by rain within this near zone can be larger than in the far zone of the pattern and, of course, power scattered in the near zone is not subject to as much attenuation in the path to the antenna.

Several models of the rain environment are discussed to greater and lesser extents. An obvious model is one of uniform rain extending over the entire path between and beyond both stations; this is referred to as Case I in the text. However, this is an unrealistic model where very high rain rates are involved because very heavy rainfall occurs in showers that are quite localized spatially.⁵ A more realistic model for heavy rains is that of a shower over only the satellite-communications antenna. This model, treated in Cases II and III, obviates the effect of attenuation over the whole path, which is quite dominant in the case of uniform rain. Case IV, the one that produces the largest coupling between the stations, involves a wall of rain which approaches the satellite communication antenna from along a line which is an

extension of the path beyond that antenna. Since the radiation patterns of both antennas look toward this wall of rain, the effect of attenuation is small.

The computations have been made for rain rates up to 400 mm/hr. The largest coupling occurs when the wall of rain is present (Case IV); this amounts to -132 dB at 4 GHz for a rain rate of 400 mm/hr and a separation of 5 km between stations and applies to cases where the level of the radiation pattern of the terrestrial radio-relay antenna (looking in the direction of the ground station) is isotropic.

It is of interest to compare the co-channel interference resulting from these couplings (of the order -140 dB) with the thermal noise level in the receiver of a typical satellite-communication ground station. Suppose the system noise temperature of a 4-GHz ground station is 70 kelvins within a 40-MHz band; the noise power referred to the input is $P_n = kT_s B$, namely -134 dBW, with the signal typically 25 dB above this value. Radio-relay systems have transmitted power rarely exceeding 10 watts; thus with -140 dB coupling, the interference level would be -130 dBW, 4 dB above the thermal noise. However, if the radio-relay antenna pattern has a sidelobe level say 10 dB above isotropic, the interference would exceed the thermal noise by 14 dB. Since in many systems it is desirable that the interference be several decibels below the thermal noise, couplings of the order -140 dB are indeed significant.

II. GENERAL ANALYSIS

Figure 1 shows a ground-station antenna (T) of a space-communications system with a beam elevated 30° (θ_1) above a path of length d to a station (R) of a terrestrial radio-relay system. The effective radius of the earth, a , and the altitude, h , at which the rain originates are also shown.

For descriptive purposes, let the ground-station be transmitting at wavelength, λ . Because of a well-tapered (quasi-gaussian) illumination, the flux on axis decreases with distance r_1 from the antenna to a volume element of the beam (see Fig. 1) in the following manner:

$$S(r_1) = \frac{E_{or_1}^2}{\eta} = \left[\frac{E_o^2}{\eta r_1^2} \right] \left[\frac{1}{r_1^2} + \left(\frac{\lambda}{\pi \bar{\rho}} \right)^2 \right]^{-1} \quad (1)$$

η being the free-space impedance and $\bar{\rho}$ the radius at which the aperture

* Thirty degrees is typical for the elevation angle of a mid-latitude station observing a synchronous satellite.

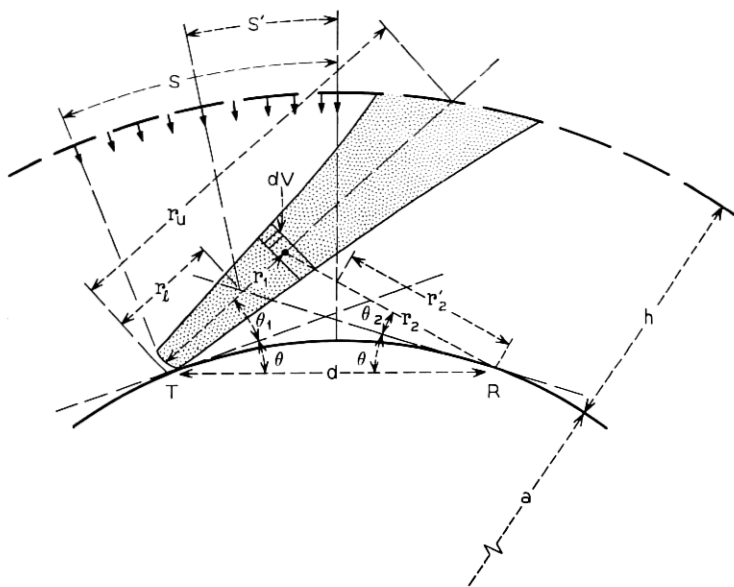


Fig. 1—Geometry of the path; $\theta_1 = 30^\circ$, $\theta = d/2a$, $a = 8500$ km, and the rain originates at height h . s and s' are dimensions of showers (see text).

field is ϵ^{-1} of its axial value, E_o . The volume element is $dV = 2\pi\rho d\rho dr_1$ where ρ is the radial coordinate of the beam. The flux at a point in the volume element is

$$S(\rho, r_1) = \frac{E_{or_1}^2}{\eta} \exp\left(\frac{-2\rho^2}{\rho_1^2}\right)$$

where ρ_1 is the radius of the annular volume element at which the field is ϵ^{-1} of its axial value (E_{or_1}). Most of the flux is contained within the beam cross section of radius ρ_1 , and ρ_1 will be used to define the boundary of the beam in what follows.

The power scattered into an antenna at R (see Fig. 1) with an effective area $A_2(\theta_2)$ in direction θ_2 toward dV is therefore

$$P_R = \int_{r_1}^{r_u} \int_0^{\rho_1} S(\rho, r_1) \frac{\sigma_v}{4\pi r_2^2} A_2(\theta_2) \exp[-\alpha(r_1 + r_2)] 2\pi\rho d\rho dr_1 \quad (2)$$

where α is the attenuation coefficient of the rain and r_2 the distance from the volume element dV to the receiver at R . The limits r_1 and r_u on r_1 depend upon the geometry of the rainstorm, and σ_v is the scattering coefficient per unit volume of the rain; these are discussed later.

Substitution of $S(\rho, r_1)$ in equation (2) and integration with respect to ρ results in

$$\int_{r_1}^{r_u} \frac{E_{or_1}^2}{\eta} \frac{\pi \rho_1^2}{2} (1 - \epsilon^{-2}) \frac{\sigma_v}{4\pi r_2^2} A_2(\theta_2) \exp[-\alpha(r_1 + r_2)] dr_1.$$

However, the gaussian beam expands such that

$$\rho_1^2 = \bar{\rho}^2 \left[1 + \left(\frac{\lambda r_1}{\pi \bar{\rho}^2} \right)^2 \right] \quad \text{and one has, using equation (1)}$$

$$P_R = \frac{E_o^2}{\eta} \frac{\pi \bar{\rho}^2}{2} (1 - \epsilon^{-2}) \int_{r_1}^{r_u} \frac{\sigma_v}{4\pi r_2^2} A_2(\theta_2) \exp[-\alpha(r_1 + r_2)] dr_1. \quad (3)$$

But the transmitted power is

$$P_T = \frac{E_o^2}{\eta} \int_0^{\bar{\rho}} \exp\left(\frac{-2\rho^2}{\bar{\rho}^2}\right) 2\pi\rho d\rho = \frac{E_o^2}{\eta} \frac{\pi \bar{\rho}^2}{2} (1 - \epsilon^{-2}).$$

Therefore, from equation (3), one obtains

$$\frac{P_R}{P_T} = \int_{r_1}^{r_u} \frac{\sigma_v}{4\pi r_2^2} A_2(\theta_2) \exp[-\alpha(r_1 + r_2)] dr_1. \quad (4)$$

Of course equation (4) takes into account the near-field zone of the ground-station antenna; equation (4) is independent of the aperture diameter of that antenna.

For the computations that follow, equation (4) was simplified in two respects. First, the response of the radio relay antenna was taken to be isotropic that is, $A_2 = \lambda^2/4\pi$, independent of θ_2 . Other cases computed consider particular configurations where the beams of typical radio-relay antennas with given radiation patterns $A_2(\theta)$ are pointed toward the space station. In some of these cases, the scattered power is simply increased by the gain of that antenna, but instances where this rule does not hold are discussed toward the end of the paper.

Secondly, the scattering by the raindrops is taken to be isotropic, and we use a relationship⁶ based upon the Laws and Parsons drop-size distribution

$$\sigma_v = 0.18 \frac{\pi^5}{\lambda^4} 10^{-15} R^{1.6} (m^{-1}),$$

R being the equivalent rain rate in millimeters per hour.* It is known that large raindrops do not scatter isotropically, especially when the

* Rigorously, one should evaluate the Stokes parameter and the differential scattering cross sections for all drops in a given rain.

operating wavelength approaches the millimeter band, but the error is not large⁶ for the wavelengths considered here. Perhaps more serious is that the drop-size distribution (and indeed the equivalent rain rates themselves) are not well determined for the upper troposphere. Here we will be guided by rain rates measured at ground level,⁷ and carry this parameter to 400 mm/hr in certain cases.

The computations are made for the frequencies 4, 6, 11, 18.5 and 30 GHz and the corresponding attenuation coefficients, α , used here (taken in part from Refs. 2 and 6) are: $0.23 \cdot 10^{-6} R^{1.1}$, $0.69 \cdot 10^{-6} R^{1.22}$, $2.5 \cdot 10^{-6} R^{1.28}$, $16 \cdot 10^{-6} R^{1.09}$ and $55 \cdot 10^{-6} R^{1.0}$, in units of inverse meters, R being in millimeters per hour.

The several sections that follow deal with various rain geometries. The rain is assumed to originate at a height, h , of four kilometers in all cases.

III. CASE I—RAIN UNIFORM OVER THE PATH BETWEEN THE TWO STATIONS

3.1 Computation

The lower and upper limits in equation (4) are

$$r_l = d \sin \theta / \sin (\theta_1 + 2\theta) \quad \text{and}$$

$$r_u = (a^2 \sin^2 \theta_1 + 2ah + h^2)^{1/2} - a \sin \theta_1$$

for this case. These limits apply specifically when one station is beyond the horizon from the other, a being the effective earth radius and θ_2 the angle between the tangent plane and the chord between the stations as shown in Fig. 1. In the event the two stations are within line-of-sight of one another, the above limits reduce to

$$r_l = 0 \quad \text{and} \quad r_u = h / \sin \theta_1 .$$

Computations have been made using both sets of limits (for this case $r_2 = |r_1^2 + d^2 - 2r_1 d \cos (\theta_1 + \theta)|^{1/2}$). At the distances of transition from line-of-sight to beyond-horizon conditions ($d > 50$ km) the data are found to behave properly.

3.2 Results

Plots of coupling between T and R are shown in Figs. 2a through e for the frequencies 4, 6, 11, 18.5 and 30 GHz, interstation separation being a parameter. The abscissa is the equivalent rain rate in millimeters per hour, assumed uniform between stations to a height of four kilometers.

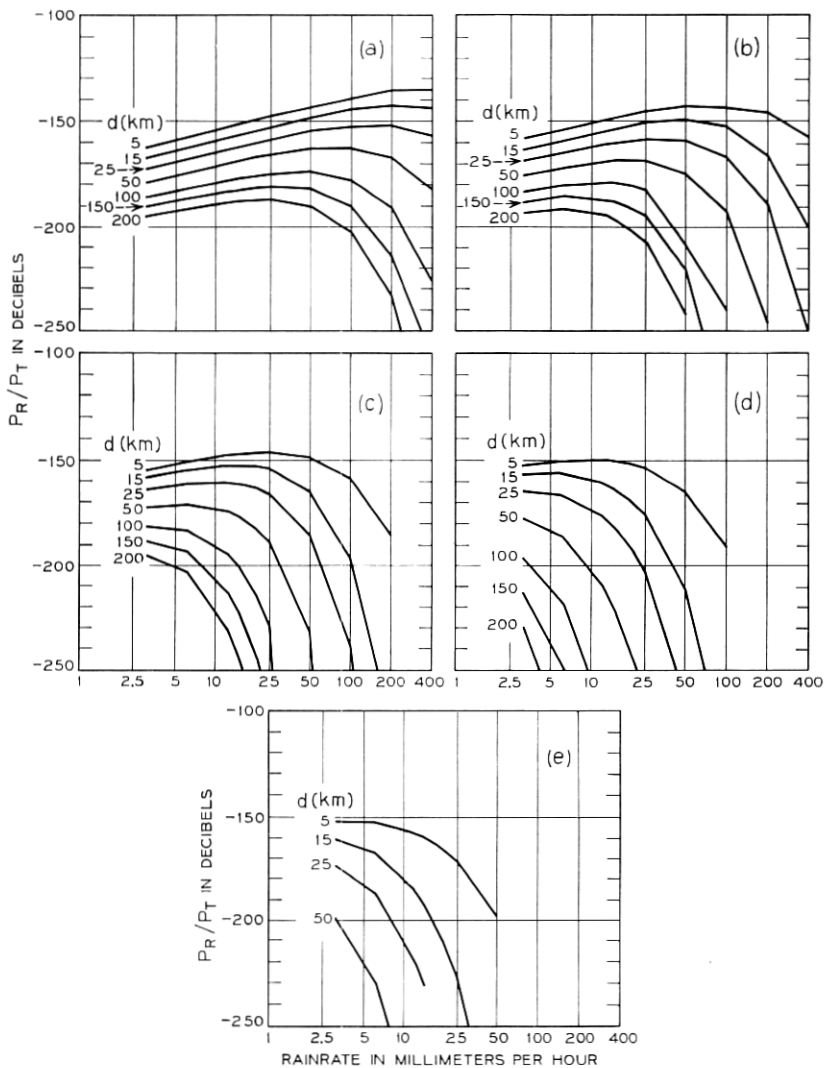


Fig. 2—Coupling for uniform rain originating at a height $h = 4$ km versus rain rate; elevation of ground-station antenna beam is 30° ; isotropic antenna at R . (a) 4 GHz, (b) 6 GHz, (c) 11 GHz, (d) 18.5 GHz, and (e) 30 GHz.

The curves of Fig. 2 are computed for $A_2(\theta) = \lambda^2/4\pi$ in equation (4); that is, for an isotropic receiving antenna at R . * Data for an antenna with a gain of the order 40 dB beamed from R toward T have also been computed; in this case, often one need only add the gain of the antenna (in decibels) to the curves of Fig. 2, a procedure discussed in more detail in Section VII.

An obvious characteristic of the curves in Fig. 2 is that they possess a maximum. As one proceeds from Fig. 2a through e (4 GHz to 30 GHz) the maxima move to ever lower rain rates. This feature evidences the effect of attenuation. Likewise for a given set of curves (Fig. 2a, for example) the maximum occurs at ever lower rain rates as the path length increases, as one would expect in an attenuating medium.

Although these results for uniform rain are instructive, some of them represent situations which do not occur in nature. For example, it is possible that rain rates of the order 200 mm/hr occur over a 5 km path; but it is highly unlikely (or impossible⁷) that such high rates occur over a path of length 200 km. Thus the high rain rate and long path length portion of the data in Fig. 2 should be considered somewhat academic. At the higher frequencies this portion of the data is of little significance anyway (Fig. 2d, for example).

The maximum value of the coupling for Case I appears in Fig. 2a (4 GHz) for the shortest interstation distance (5 km) and the highest rain rate considered (400 mm/hr); it is -136 dB. But maxima of the order -150 dB occur for higher frequencies and the same pathlength at lower rain rates.

IV. CASE II—LOCALIZED SHOWER AT THE SATELLITE STATION

4.1 Computation

As shown in Fig. 1, one can introduce another parameter, s , which defines the extent of a shower along the path from the ground-station T toward R . As discussed above, very heavy rainfall is spatially restricted, therefore Case II is more realistic than Case I in the high rain rate regime.

For computation of Case II, both the limits on r_1 and the exponent of the exponential in equation (4) must be modified, the latter because much of the path (r_2) from R to the beam of the ground-station antenna no longer introduces attenuation, the rain being localized near T . Let r'_2 be that portion of r_2 with no precipitation. Then the exponent in

* Representative of the case where the back or far side lobes of a radio-relay antenna are directed toward the ground station.

equation (4) becomes $-\alpha(r_1 + r_2 - r'_2)$ where

$$r'_2 = d \frac{\left[\sin^2 \theta - \frac{1}{\cos \theta} + \frac{s}{d} \right]}{\left[\sin^2 \theta + \frac{1}{\cos \theta} + \sin \theta \sin (\theta + \theta_2) \right] \cos (\theta + \theta_2)} .$$

The limits in equation (3) for this case are

$$r_i = d \sin \theta \sin (\theta_1 + 2\theta) \quad \text{and} \quad r_u = s/\cos \theta_1$$

which for line-of-sight conditions ($\theta = 0$) reduce to

$$r_i = 0, \quad \text{and} \quad r_u = s/\cos \theta_1 .$$

In both cases r_u , and also the effective height of the shower, depend upon its lateral extent, s . Again, the computations show that the transition from line-of-sight to beyond-horizon conditions is well behaved. The expression for r_2 is given in Section III.

4.2 Results

Plots of coupling for this case are given in Figs. 3a through e, the antenna at R again being taken to be isotropic. The shower has an extent one kilometer along the path from T and a height of 4 kilometers.

At the higher frequencies in Fig. 3 maxima in the coupling appear, somewhat as in Fig. 2, but the former occur at much higher rain rates than the latter. For example, at 11 GHz, the maxima in Fig. 3c are at about 100 mm/hr, whereas in Fig. 2c no maximum occurs above the rain rates of 25 mm/hr. Since one is dealing with a localized shower it is not surprising that the effect of attenuation sets in at rain rates higher in Fig. 3 than in Fig. 2.

The maximum value attained by the coupling is about -135 dB as shown at 400 mm/hr on Figs. 3a and b for an interstation separation of 5 km. However, maxima of the order -140 dB occur in Figs. 3c through 3e at lesser rain rates.

A feature of the data in Fig. 3 is that the coupling decreases drastically as the distance increases from 50 to 100 km. This decrease is associated with the effective height of the shower, as governed by its width s ; beyond $d = 50$ km the scattering volume decreases rapidly. Computations not shown here have been made for showers of lateral extent up to 8 km and, as one would expect, such data lie between those of Figs. 2 and 3. As the extent of the shower increases, the rapid decrease in coupling for distances beyond 50 km becomes less marked.

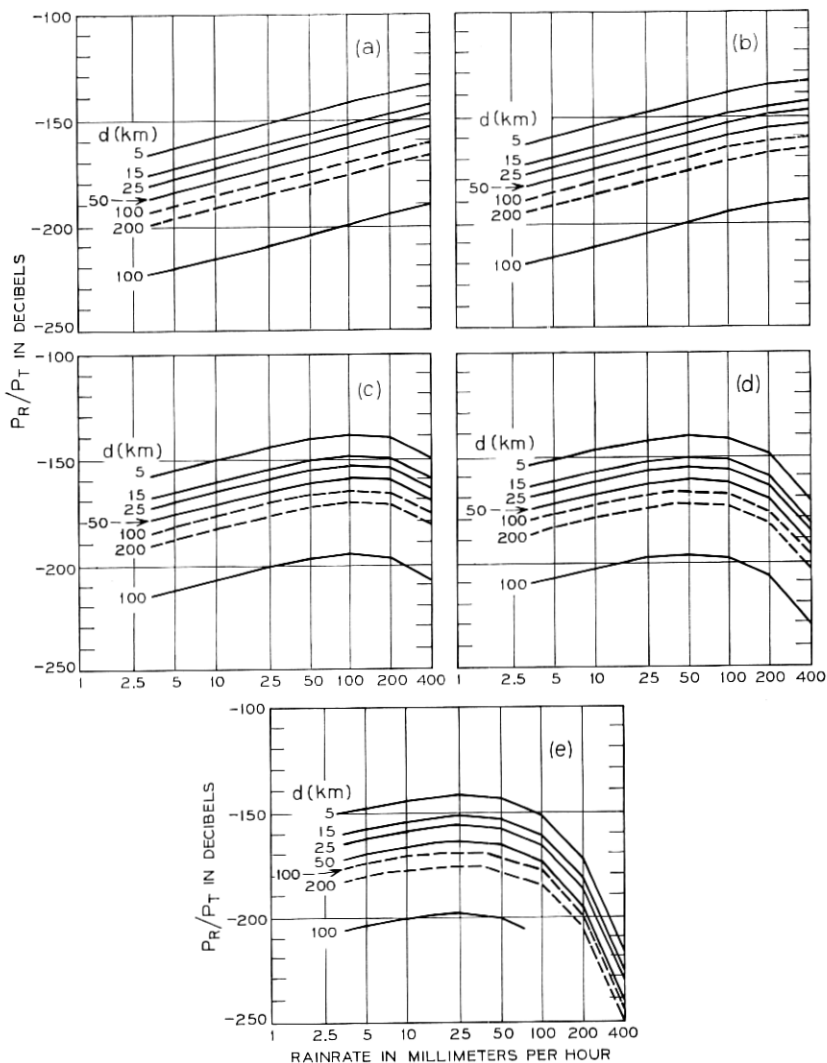


Fig. 3—Coupling for a shower ($S = 1$ km) originating at a height of 4 km above ground station (T) versus rain rate; elevation of ground-station antenna beam is 30° ; isotropic antenna at R . (a) 4 GHz, (b) 6 GHz, (c) 11 GHz, (d) 18.5 GHz, (e) 30 GHz. The dashed lines correspond to a shower $S' = 1$ km in extent located at the intersection of the ground-station beam and the tangent plane of the earth (see Fig. 1).

V. CASE III—LOCALIZED SHOWER AT BEAM INTERSECTION

5.1 Computation

A modification of the localized shower model (Case II) is achieved by moving the shower (extent s') along the path toward R thereby locating the rain at the intersection of the earth station beam and earth tangent at R as shown in Fig. 1. This geometry results in a scattering volume for the over-the-horizon cases ($d > 50$ km) much larger than that considered in Case II while retaining the limited rain extent.

For the computations of Case III, the lower limit in equation (4) again becomes

$$r_l = d \sin \theta / [\sin (\theta_1 + 2\theta)].$$

The upper limit for this case depends upon whether the earth-station beam emerges from the vertical boundary of the precipitation or from the upper boundary defined by h .

Introducing two new parameters θ' and θ'' where

$$\theta' = 2\theta - \tan^{-1} \{ [r_1^2 + d^2 - 2r_1 d \cos (\theta_1 + \theta)]^{1/2} / a \}$$

and

$$\theta'' = s'/a,$$

the upper limit where the beam emerges from the vertical boundary is

$$r_u = a \sin (\theta' + \theta'') / \cos (\theta_1 + \theta' + \theta''),$$

or where the beam emerges from the upper boundary

$$r_u = (a^2 \sin^2 \theta_1 + 2ah + h^2)^{1/2} - a \sin \theta_1.$$

For computational purposes, the smaller upper limit is the correct value for a given set of conditions. The path length r_2 from the differential scattering volume is given by

$$r_2 = [r_1^2 + d^2 - 2r_1 d \cos (\theta_1 - \theta)]^{1/2}.$$

The exponent in equation (4) must also be further modified because portions of both r_1 and r_2 no longer introduce attenuation. Let r'_1 and r'_2 be those portions of r_1 and r_2 with no precipitation. The exponent in equation (4) then becomes $-\alpha(r_1 + r_2 - r'_1 - r'_2)$ where

$$r'_1 = r_l,$$

$$r'_2 = [a \sin (2\theta - \theta' - \theta'') / \cos (\theta_2 + 2\theta - \theta' - \theta'')],$$

and

$$\theta_2 = \sin^{-1} \{[(r_1 - r_i) \sin (\theta_1 + 2\theta)]/r_2\}$$

is the elevation angle between r_2 and the tangent plane at R .

5.2 Results

The coupling for distances of 100 and 200 km is shown with the data for Case II as broken lines in Figs. 3a through e, the conditions being identical to Case II except for the lateral displacement of the rain region to the beam intersection. The coupling for distances of 50 km or less have been omitted since the results and configurations are essentially the same as Case II for line-of-sight conditions of 50 km or less.

Comparing the results for Case II and III, the coupling at distances greater than 50 km is greatly increased over the corresponding results for Case II due to the larger scattering volume. At distances greater than 200 km, the scattering volume would be limited by the assumed rain height of 4 km and one would expect a drastic decrease in coupling beyond 200 km.

VI. CASE IV—A WALL OF RAIN NORMAL TO THE PATH EXTENDED BEYOND THE SATELLITE STATION

6.1 Computation

In cases I through III, the region of rain is located on the path between the ground station and the relay station (Fig. 1). However, "off-path" orientations of the ground-station beam relative to the terrestrial radio-relay station are typical of actual system configurations. We examine one such "off-path" orientation in which the ground-station beam points directly away from the radio relay in azimuth. The region of rain is then located on the path extended beyond the earth station, and the energy may be scattered from the boundary of the rain without additional attenuation on the path to the relay station.

The model used for analysis is shown in Fig. 4. A wall of rain normal to the path is located at the intersection of the axis of the ground-station beam and the earth tangent plane from the relay station.

For computation of this case, the limits in equation (4) become

$$r_i = d \sin \theta / \sin (\theta_1 - 2\theta)$$

and

$$r_u = (a^2 \sin^2 \theta_1 + 2ah + h^2)^{1/2} - a \sin \theta_1 .$$

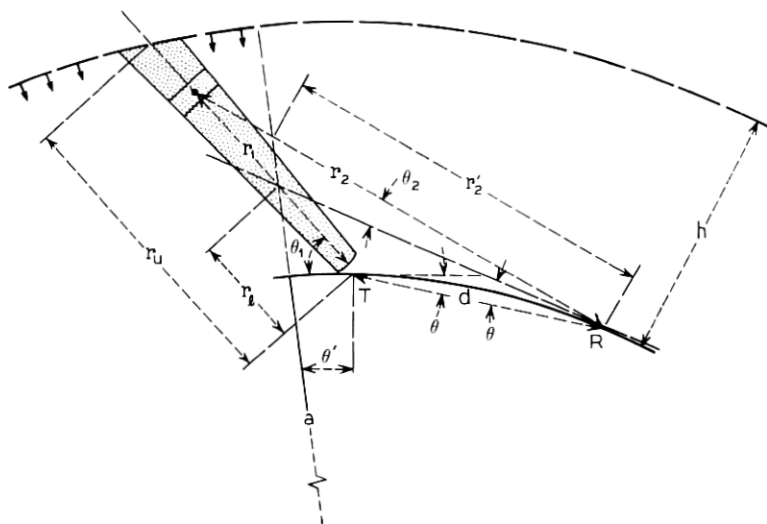


Fig. 4—Geometry for a rain originating at altitude h on the path extended beyond T ; $\theta_1 = 30^\circ$, $\theta = d/2a$, $a = 8500$ km.

The path length r_2 from the differential scattering volume is given by

$$r_2 = [r_1^2 + d^2 + 2r_1 d \cos(\theta_1 - \theta)]^{1/2}.$$

The portions of paths r_1 and r_2 with no precipitation, r'_1 and r'_2 are given by

$$r'_1 = r_1 - r_i$$

$$r'_2 = a \sin(\theta' + 2\theta) \cos(\theta' + 2\theta + \theta_2)$$

where the angles θ_2 and θ' (Fig. 4) are

$$\theta_2 = \sin^{-1} \{[(r_1 - r_i) \sin(\theta_1 - 2\theta)]/r_2\}$$

and

$$\theta' = \tan^{-1} \{[r_1^2 + d^2 + 2r_1 d \cos(\theta_1 - \theta)]^{1/2}/a\} - 2\theta.$$

As for Case III, the exponent in Equation (4) then becomes

$$-\alpha(r_1 + r_2 - r'_1 - r'_2).$$

6.2 Results

Plots of the coupling for the extended path scattering are shown in Figs. 5a through e for a rain height of 4 km and earth station elevation

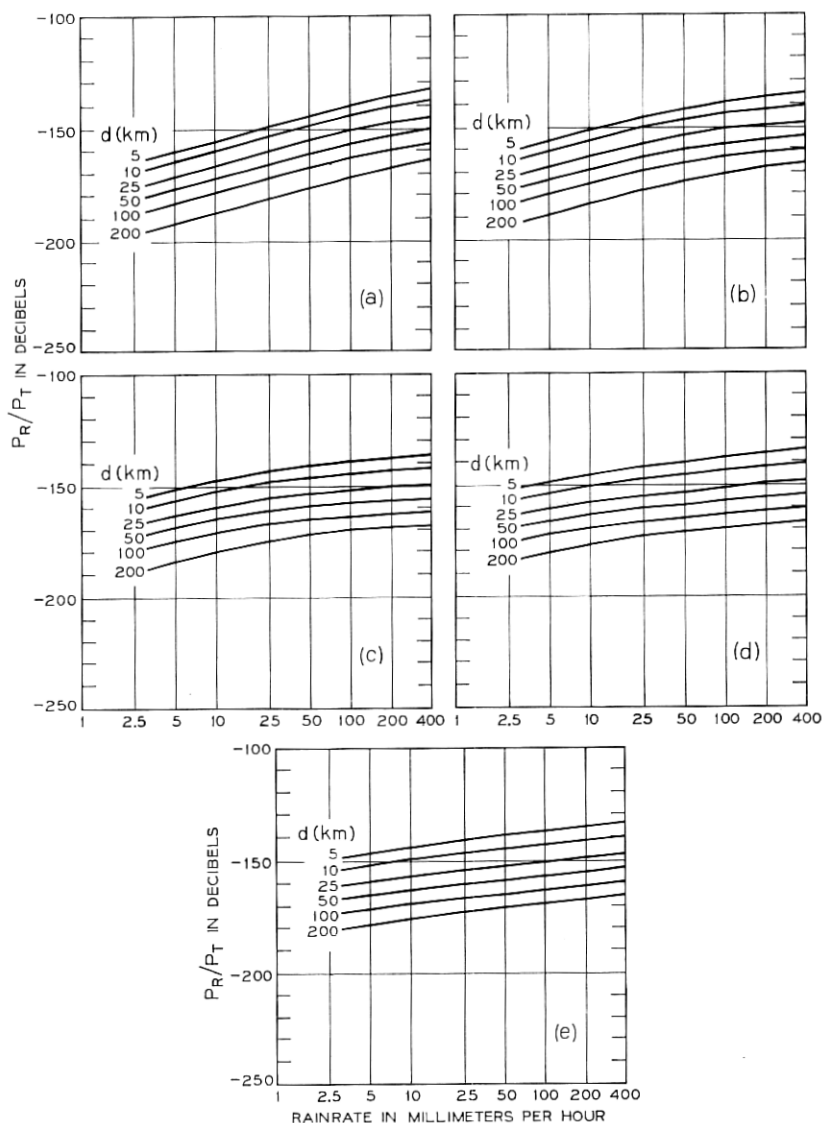


Fig. 5—Coupling for rain originating at a height $h = 4$ km on the extended path versus rain rate; elevation of ground-station antenna beam is 30° ; isotropic antenna at R . (a) 4 GHz, (b) 6 GHz, (c) 11 GHz, (d) 18.5 GHz, (e) 30 GHz.

of 30 degrees. The most notable feature is that the coupling increases with rain rate for all frequencies over the range of rain rates considered. This is in contrast with the previous cases where the curves possessed a maximum at the higher frequencies.

Maximum coupling, approximately -132 dB, occurs at 4 GHz for a separation of 5 km and a rain rate of 400 mm/hr. However, the coupling is reasonably independent (within about 4 dB) of frequency for rain rates greater than about 100 mm/hr. At lower rain rates, the coupling increases with frequency as one would expect; for example, at 5 mm/hr and 100-km separation, the coupling is about -183 dB at 4 GHz and -171 dB at 30 GHz.

VII. EFFECT OF DIRECTIVE ANTENNAS

The effect of the directivity of typical terrestrial radio-relay antennas on the coupling has been computed for all cases treated above. For each case, the beam of the radio relay antenna is assumed to be directed toward the ground station, that is, along the horizon plane (dashed) in Figs. 1 and 4. This is a very pessimistic condition and one hopefully not encountered too often in practice.

The response pattern of the radio-relay antenna $A_2(\theta_2)$ in equation (4) is assumed to be of the form

$$A_2(\theta_2) = A_o[\exp(-K_1\theta_2^2) + \exp-(K_2 + K_3\theta_2)], \quad (5)$$

θ_2 being the angle measured in degrees from the axis of the relay station beam and A_o the effective area. The first term in equation (5) is the familiar gaussian approximation for the main beam. The second term represents the envelope of the far side lobes of the pattern using constants K_2 and K_3 of 5.5 and 0.115 respectively.

At 4 and 6 GHz, the radio relay antenna is assumed to have a beamwidth of one degree ($K_1 = 2.8$) with 43 dB gain. At 11, 18 and 30 GHz, the beamwidth is taken to be two and a half degrees ($K_1 = 0.41$) with 36 dB gain.

In what follows, the gain realized or coupling relative to the isotropic case is plotted versus rain rate. Thus, the coupling for the directive case is obtained by adding the gain realized to the coupling for the corresponding isotropic case; thus, if the gain realized is 30 dB and the isotropic coupling is -130 dB, the coupling in the directive case is -100 dB.

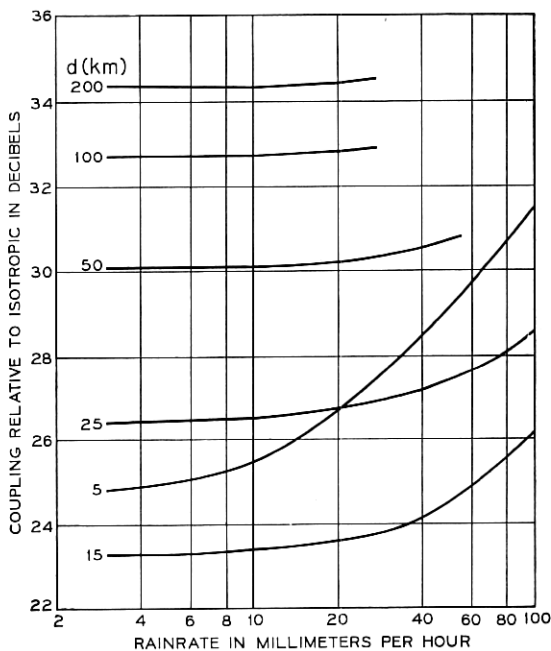


Fig. 6—Coupling for an antenna with 36 dB gain located at R and directed toward T relative to an isotropic antenna at R (gain realized) versus rain rate; frequency 11 GHz.

7.1 Uniform Rain (Case I)

The effect of directivity at 11 GHz is shown in Fig. 6 where the coupling relative to the isotropic case (gain realized*) is plotted versus rain rate for various separations between the ground-station and terrestrial radio-relay antennas. It is clear that at low rain rates most of the nominal gain is realized for the larger separations. At 100 to 200 km separation, the beam of the radio-relay antenna illuminates about the same volume as does an isotropic antenna, the volume in this case being limited by the horizon plane and the upper boundary of the rainstorm (see Fig. 1). But as the separation is decreased to, say, 25 km, Fig. 6 shows that the gain realized is decreased by about 10 dB, the intersections of the ground-station and radio-relay beams define the effective volume whereas an isotropic antenna at R would see essentially all of the ground-station beam.

* Of course, antenna gain is a constant but the concept of gain realized in propagating through a given medium is convenient and will be used here.

Figure 6 also shows that the gain realized increases with rain rate, especially for the lesser separations. This is caused by attenuation of the signal scattered from the further (upper) portions of the ground-station beam (see Fig. 1) which, for heavy enough rain rates, produces an effective scattering volume (for an isotropic antenna at R) which is not too much larger than the volume defined by the two beams in the directive case.

A somewhat more subtle effect is the minimum in gain realized which occurs at some separation between 5 and 25 km in Fig. 6. For example, at a rain rate of 50 mm/hr, the gains realized at separations of 50, 25, 15 and 5 km are 31, 27, 24 and 29 dB. Thus, the gain realized begins to increase when the separation is decreased below about 10 km. Now the axis of the beam directed toward space intersects the upper boundary of the rain at a distance of about 7 km along the earth's surface from the ground station and it is at this separation that the total path from R to the upper portions of the volume occupied by the beam (see Fig. 1) is a minimum; that is, r_2 for the upper portions of the beam is a minimum at $d \simeq 7$ km. Thus, for $d < 7$ km the effective volume for an isotropic antenna at R is further decreased and the gain realized with a directive antenna (relative to the isotropic case) increases. For these small separations, the gain realized also increases with rain rate as discussed in the previous paragraph.

At 18 and 30 GHz, the behaviour of the data is similar to that of Fig. 6 but the effect of attenuation is so high that the curvatures are more pronounced. At 4 and 6 GHz, the antenna gain is realized and is relatively independent of separation and rain rate.

7.2 *Extended Path (Case IV)*

The results for the extended path scattering are shown in Fig. 7 for (a) 4 and 6 GHz and (b) 18.5 GHz. As in the previous case, the gain realized is nearly equal to the nominal gain at the maximum separation distance of 200 km where the common volume is not limited by the relay antenna beamwidth. For lesser separations, the gain realized decreases depending on both the separation and rain rate. The gain realized at the shortest distance (5 km) is reduced below the nominal gain by a maximum of about 15 dB at 4 and 6 GHz and about 11 dB at 18 GHz the 4 dB difference corresponding to the ratio of the assumed beamwidths of one degree at 4 and 6 GHz and two and one half degrees at 18 GHz.

The gain realized at low rain rates with small separations is somewhat larger than in Case I. For example, the gain realized at 18 GHz

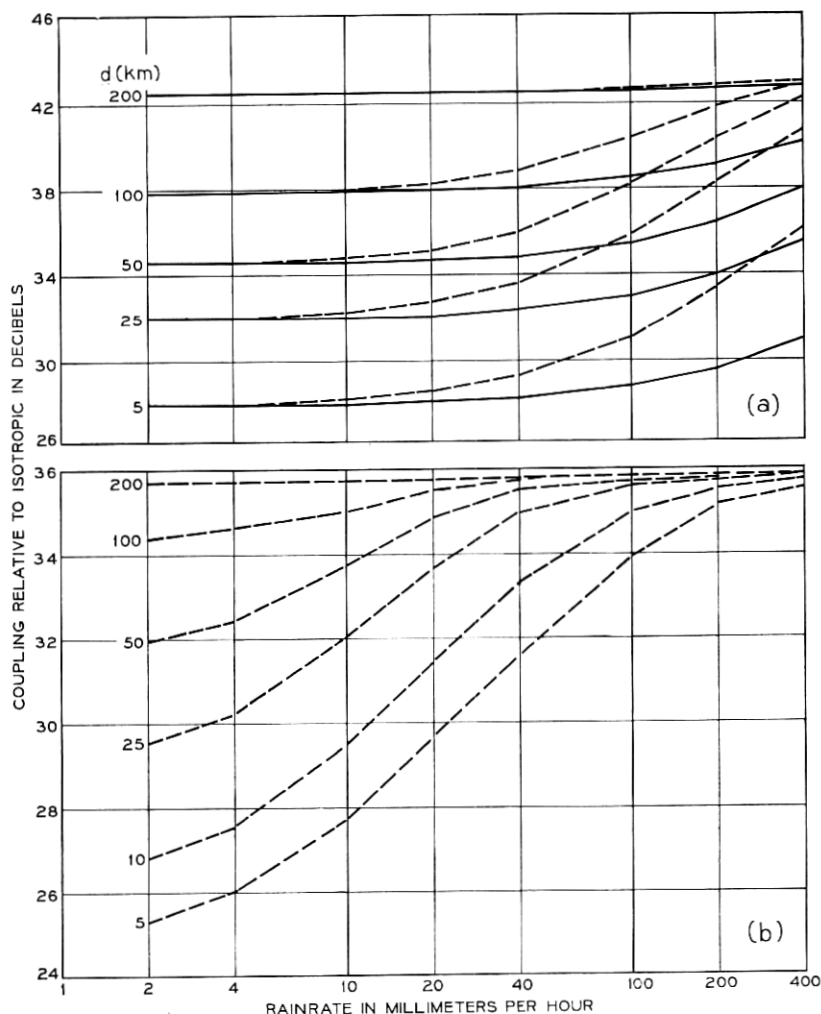


Fig. 7—(a) Coupling for an antenna with 43 dB gain located at R and directed toward T relative to an isotropic antenna at R (gain realized) versus rain rate; frequencies 4 and 6 GHz. (b) Coupling for an antenna with 36 dB gain located at R and directed toward T relative to an isotropic antenna at R (gain realized) versus rain rate; frequency 18 GHz.

and 3 mm/hr (Fig. 7b) with 25 km separation is about 6 dB below the nominal gain whereas the reduction for the Case I (Fig. 6) is 10 dB below nominal. In Case IV, the directive radio relay antenna confines the significant volume to the lower region of the rain; but the significant volume where the isotropic antenna is involved is also near the ground station antenna because r_2 is a minimum there. On the other hand, in Case I, the upper portion of the isotropic scattering volume contributes significantly as discussed in the previous section.

In Case IV, the gain realized also increases with attenuation and hence rain rate as shown in Fig. 7 because the attenuation decreases the effective depth of the isotropic scattering volume. For very high attenuation, most of the energy is scattered from that volume of the rain nearest the ground station and the gain realized is approximately equal to nominal gain; for example, the gain realized is within 2 dB of the nominal gain for rain rates greater than 100 mm/hr at 18 GHz (Fig. 7).

The plots of the gain realized at 11 and 30 GHz (not shown here) are within ± 3 dB of the 18 GHz curves, the gain realized being greater at 30 GHz and smaller at 11 GHz. The maximum deviation occurs at 5 km and decreases with increasing separations. At 50 km, the difference is ± 2 dB and decreases to only ± 1 dB at 100 km.

VIII. DISCUSSION AND SPECIAL EFFECTS

What does all of this mean in terms of what happens in a real-life situation? The various models which have been presented do not represent all the possible orientations and rain conditions that would exist in real situations; however, the coupling caused by realistic rainstorms should range between the results for localized showers (Cases II, III, IV) and those for uniform rain (Case I), depending of course on the spatial distribution of the rain over the path. At 4 and 6 GHz, the effects of rain attenuation are small, at least for realistic sizes of areas with high rain rate, and the results for Cases II and III give a good estimate of the coupling which might be expected for a given rain rate in the ground-station antenna beam. Thus, couplings of the order -140 dB at 5 km to -170 dB at 200 km (Fig. 3a and b) for an isotropic level response at the relay station are typical at 4 and 6 GHz for rain rates of 100 mm/hr or greater.

At frequencies above 10 GHz, attenuation by the rain over the entire path is a dominant factor and it gives rise to large variations in the coupling for the various cases considered. For example, the

coupling at 30 GHz for a uniform rain of 10 mm/hr over a 25 km path (Case I) is -210 dB, whereas, the corresponding coupling with localized showers is -175 dB and -160 dB for Cases II and IV, respectively. However, the maximum couplings with localized showers are about the same as the couplings at 4 and 6 GHz. Thus the spatial distribution of rainfall is an important factor in evaluating the potential interference coupling due to scatter by rain in future systems which may use frequencies exceeding 10 GHz.

Satellite systems above 10 GHz will no doubt use a diversity system of two or more earth stations spaced some few miles apart to avoid outages due to attenuation by rain. Such a path-diversity system will minimize the rain-scatter interference problem since the earth station with the least attenuation and hence with the least rain in its antenna beam will carry the information-bearing signal.

Other factors which will affect the coupling due to scatter should be mentioned. First, the height of the rain for all cases has been taken to be 4 km whereas weather radar data^{8,9} show that high effective rain-rates may exist at heights of 10 km. This will extend to horizon for direct rain-scatter coupling to distances of 400 km or more. Also, polarization has been neglected in the calculation; for certain orientations of the ground-station and radio-relay antenna beams, the coupling will be decreased due to this effect.

Another important consideration is that the scattering and attenuation constants, based on empirical data in each case, are not consistent for very high rain rates. Based on these data, we have taken the scattering coefficient to increase as the 1.6 power of rain rate whereas the attenuation constant increases as a lesser power; this gives an inconsistent result at 30 GHz for rain rates greater than about 100 mm/hr in that the attenuation is less than the power lost due to the predicted scatter! Thus, at 30 GHz, and high rain rates, the scattering is less than we have calculated. At frequencies less than 30 GHz, the discrepancy is very small.

In summary, the calculated results show that couplings of the order -140 dB to -170 dB at distances of 5 km to 200 km, respectively, can be expected with an isotropic antenna response at the terrestrial radio relay station, for the small percentages of time associated with heavy rain rates.* These couplings are increased significantly if the response of the relay station exceeds isotropic in the general direction of the earth station. As discussed in the introduction, since couplings

* In New Jersey, rain rates of 200 mm/hr have been observed for periods of the order five minutes during a year (0.001 percent of the time).

of the -140 dB are significant, interference due to scatter by rain is a factor which should receive consideration in locating satellite stations. Of course, direct coupling via antenna side lobes and coupling via tropospheric scatter must also be taken into account. In essentially all cases considered here, the coupling due to scatter by rain is less than the line-of-sight coupling but exceeds the median tropospheric scatter coupling between isotropic antennas at the two stations.

There are several previous publications concerned with interference caused by scattering from precipitation¹⁰⁻¹⁴ but experimental data are sparse. We find agreement between the present calculations and the limited data given in Refs. 10 and 12.

IX. ACKNOWLEDGMENT

Mrs. C. L. Beattie did much of the initial computation. The question of interference due to scattering by rain at frequencies exceeding 10 GHz was raised by J. B. Fisk.

REFERENCES

1. Proceedings of the Thirteenth Radar Meteorology Conference, American Meteorological Society, McGill University, Montreal, Canada, August, 1968.
2. Semplak, R. A., and Turrin, R. H., "Some Measurements of Attenuation by Rainfall at 18.5 GHz," *B.S.T.J.*, 48, No. 6, (July-August 1969), pp. 1767.
3. Chu, T. S., "On Coherent Detection of Scattered Light," *IEEE Trans. Antennas and Propagation*, AP-15, No. 5 (September 1967), pp. 703-704.
4. Kogelnik, H., "Imaging of Optical Mode Resonators with Internal Lenses," *B.S.T.J.*, 44, No. 3 (March 1965), p. 455, equation (50).
5. Freeny, A. E., and Gabbe, J. D., "A Statistical Description of Intense Rainfall," *B.S.T.J.*, 48, No. 6 (July-August 1969), p. 1789.
6. Gunn, K. L. S., and East, J. W. R., "The Microwave Properties of Precipitation Particles," *J. Royal Meteorological Soc.*, 80, (1954), pp. 522-545.
7. Hogg, D. C., "Statistics on Attenuation of Microwaves by Intense Rain," *B.S.T.J.*, 48, No. 9 (November 1969), pp. 2949-2962.
8. Marshall, J. S., Holtz, Clifford D., and Weiss, Marianne, "Parameters for Airborne Weather Radar," Scientific Report MW-48, Stormy Weather Group, McGill University, Montreal, Canada, May 1965.
9. Atlas, D., "Model Atmospheres for Precipitation," *Handbook for Geophysics and Space Environments*, Bedford, Massachusetts: Air Force Cambridge Research Laboratories, 1965, Section 5.2, p. 6.
10. Hogg, D. C., Semplak, R. A., and Gray, D. A., "Measurement of Microwave Interference at 4 Ge Due to Scatter by Rain," *Proc. IEEE*, 51, No. 3 (March 1963), p. 500.
11. Dennis, A. S., "Forward Scatter From Precipitation as an Interference Source at Stations Monitoring Satellites," Stanford Res. Memo 2, Project 3773, November 1961.
12. Buige, A., and Levatich, J. L., "Measurement of Precipitation Scatter Effect on Propagation at 6, 12 and 18 GHz," to be published AIAA Conference Proceedings, Los Angeles, California, April, 1970.
13. Altman, F. J., "Design of a Precipitation Scatter Experiment," URSI—Fall Meeting, Austin, Texas, December, 1969.
14. Carey, R. B., and Kalagain, G. S., "Detailed Analysis of FCC/USAF POPSI Project Data," URSI—Fall Meeting, Austin, Texas, December 1969.

